Letter

Selective A₃ Adenosine Receptor Antagonist Radioligand for Human and Rodent Species

R. Rama Suresh, Zhan-Guo Gao, Veronica Salmaso, Eric Chen, Ryan G. Campbell, Russell B. Poe, Theodore E. Liston, and Kenneth A. Jacobson*

Cite This: ACS Med. Chem. Lett. 2022, 13, 623−631   Read Online

ACCESS | 📊 Metrics & More | 📖 Article Recommendations | 🆘 Supporting Information

ABSTRACT: The A₃ adenosine receptor (A₃AR) is a target for pain, ischemia, and inflammatory disease therapy. Among the ligand tools available are selective agonists and antagonists, including radioligands, but most high-affinity non-nucleoside antagonists are limited in selectivity to primate species. We have explored the structure−activity relationship of a previously reported A₃AR antagonist DPTN **9** (N-[4-(3,5-dimethylphenyl)-5-(4-pyridyl)-1,3-thiazol-2-yl]nicotinamide) for radiolabeling, including 3-halo derivatives (3-iodo, MRS7907), and characterized **9** as a high-affinity radioligand [³H]MRS7799. A₃AR K_d values were (nM): 0.55 (human), 3.74 (mouse), and 2.80 (rat). An extended methyl acrylate (MRS8074, **19**) maintained higher affinity (18.9 nM) than a 3-((5-chlorothiophen-2-yl)ethynyl) derivative **20**. Compound **9** had an excellent brain distribution in rats (brain/plasma ratio ∼1). Receptor docking predicted its orthosteric site binding by engaging residues that were previously found to be essential for AR binding. Thus the new radioligand promises to be a useful species-general antagonist tracer for receptor characterization and drug discovery.
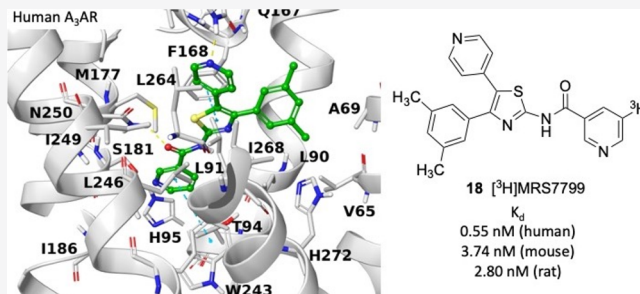
KEYWORDS: Adenosine receptor, G-protein-coupled receptor, antagonist, molecular dynamics, radioligand

The G_i-coupled A₃ adenosine receptor (A₃AR) is a therapeutic target of interest in pain, neurodegeneration, cancer, ischemia of the heart and brain, autoimmune inflammatory diseases, and other conditions.[1−8] In humans, the A₃AR is expressed highly in the lung, liver, kidney, and heart. Two A₃AR agonists are in advanced clinical trials for psoriasis, COVID-19, hepatocellular carcinoma (HCC), and nonalcoholic steatohepatitis (NASH).[1,3,9] A₃AR agonists are being explored for the treatment of chronic neuropathic pain, stroke, and other nervous system conditions.[7,10,11] The moderately selective A₃AR agonists already in clinical trials are IB-MECA **1** and Cl-IB-MECA **2** (Chart 1). However, we have recently expanded the A₃AR agonist structure−activity relationship (SAR) to include more highly selective (N)-methanocarba (bicyclo[3.1.0]hexyl) agonists such as **4**.[7,12]

A₃AR ligands, in particular, antagonists, are subject to interspecies differences in affinity.[13−16] Thus many of the reported highly selective human (h) A₃AR antagonists, such as [1,2,4]triazolo[1,5-c]quinazolin-5-amines and 1,4-dihydropyridines, are not at all or are marginally A₃AR-selective in rats and mice. Furthermore, the most widely used agonist radioligand, [¹²⁵I]I-AB-MECA **3**, is only slightly selective for that subtype, although it has a ∼1 nM K_d value at the rat A₃AR.[17] Efforts to use [¹²⁵I]**3** for autoradiography to exclusively label the A₃AR in brain tissue were problematic because it requires the addition of a selective A₁AR antagonist

to remove that component of binding. Other nucleoside radioligands reported include ⁷⁶Br derivatives for A₃AR positron emission tomography (PET) studies.[18] [¹²⁵I]-MRS1898 **5** proved to be a selective A₃AR agonist radioligand in binding experiments (K_d 0.17 nM, rat A₃AR).[19] Antagonist radioligands [³H]MRS3008F20 **7** and [³H]PSB11 **8** are suitable only for the primate A₃AR, as their affinities at the mouse (K_i > 10 and 6.36 μM, respectively) and rat (r) A₃ARs (both: K_i > 10 μM) were much weaker.[13] A pyridine derivative **6** is currently the best general purpose A₃AR antagonist for use in the mouse (K_i 349 nM) or rat (K_i 216 nM).[13,20] It has proven selective in various in vivo studies to define the action at the A₃AR.[7] However, efforts to convert this pyridine series into a radioligand, specifically a ¹⁸F PET ligand in the form of a closely related analogue, FE@SUPPY (not shown), were also not straightforward chemically or pharmacologically.[21] A new chemotype (5-(4-chlorophenyl)thiophene-2-carboxamide) in moderately potent hA₃AR and rA₃AR antagonists was recently

Chart 1. Select Ligands and Radioligands Used to Study the A₃AR[a]

agonists

1 R=H, IB-MECA (Piclodenoson, CF101)
2 R=Cl, Cl-IB-MECA (Namodenoson, CF102)
3 I-AB-MECA
4 MRS5980
5 MRS1898

antagonists

6 MRS1523
7 MRE3008-F20
8 PSB-11
9 DPTN
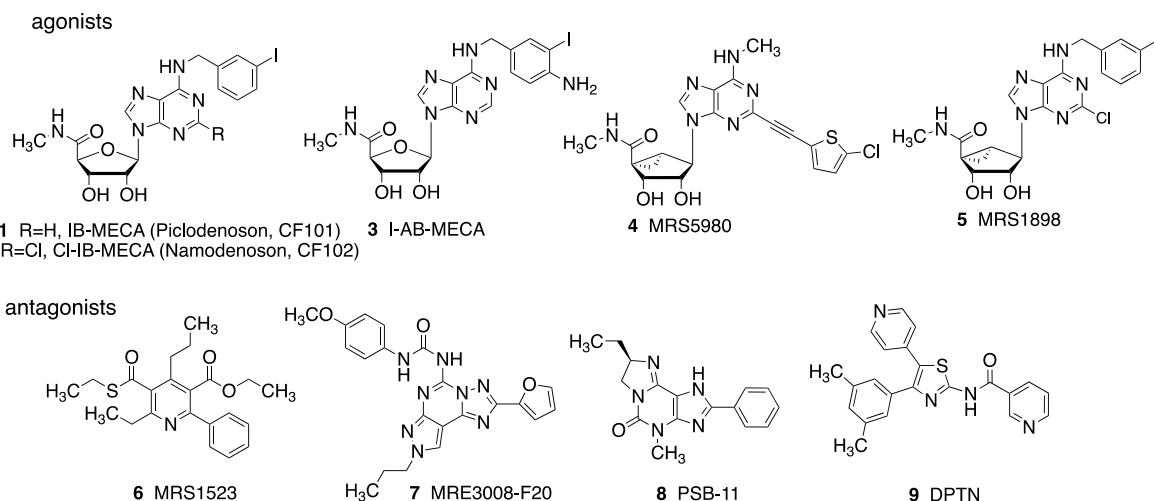
[a]Agonists **3** and **5** are used in radioiodinated form, and antagonists **7** and **8** have been tritiated. Binding K_i values at the hA₃AR (nM) are: **1**, 1.8; **2**, 1.4; **3**, ~1; **4**, 0.70; **5**, 1.4; **6**, 43.9; **7**, 1.13; **8**, 3.51.[1,13]

Scheme 1. Synthesis of Halo Analogues of 9 and Its Tritiated Form 18[a]

A

R¹ = F, **10b**
  = Br, **10c**
  = I, **10d**

R¹ = Me, **11a**
  = F, **11b**
  = Br, **11c**
  = I, **11d**

R¹ = Me, **12a**
  = F, **12b**
  = Br, **12c**
  = I, **12d**

R¹ = Me, **13a**
  = F, **13b**
  = Br, **13c**
  = I, **13d**

R¹ = Me, **14a**
  = F, **14b**
  = Br, **14c**
  = I, **14d**

R¹ = Me, **15a**
  = F, **15b**
  = Br, **15c**
  = I, **15d**

R¹ = Me, **9** (DPTN)
  = F, **16b**
  = Br, **16c**
  = I, **16d**

B

15a

17

18 [³H]MRS7799
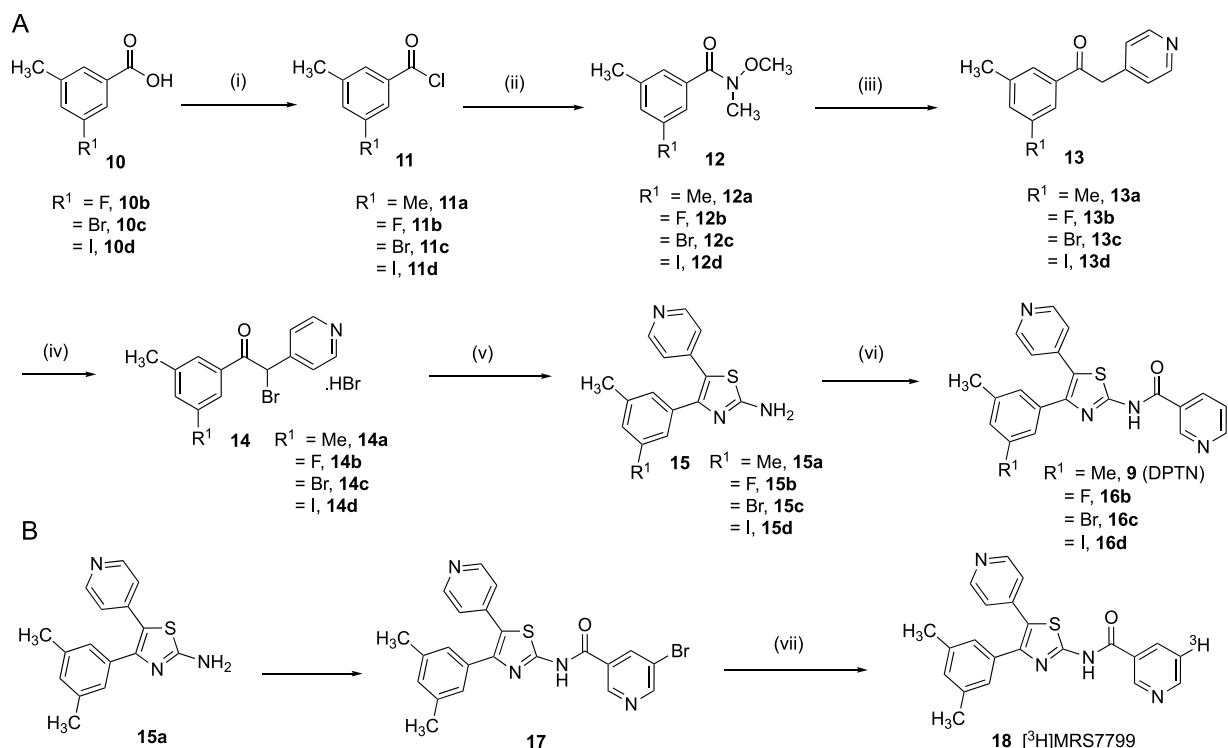
[a]Reagents and conditions: (i) (COCl)₂ (1.5 to 2.0 equiv), cat. DMF (10 μL), toluene, 0 °C to room temperature, 89−96%; (ii) N,O-dimethylhydroxylamine hydrochloride (1.2 to 1.5 equiv), K₂CO₃ (2.0 equiv), EtOAc−H₂O (2:1), 0 °C to room temperature, 16−18 h, 86−98%; (iii) 4-picoline (1.2 to 1.5 equiv), LDA (1.0 M in THF/hexane (1.0−4.0 equiv), THF, −78 °C to room temperature, 2 to 3 h, 58−71%; (iv) Br₂ (1.0 equiv), AcOH, 4 h, 80 °C, 43−90%; (v) methylthiourea (1.1 equiv), Et₃N (2.1 to 3.0 equiv), ACN, reflux, 3 h, 38−87%; (vi) nicotinoyl chloride hydrochloride or 5-bromonicotinoyl chloride (1.5 equiv), DMAP (0.3 equiv) in DMA or NMP, 80 °C, 16 h; sat. NaHCO₃, 39−87%; (vii) Pd/C, tritium gas.

reported, but it does not have sufficiently high affinity for use as a rA₃AR radioligand.[22]

We recently resynthesized an antagonist, DPTN **9** (N-[4-(3,5-dimethylphenyl)-5-(4-pyridyl)-1,3-thiazol-2-yl]-nicotinamide), as reported in 2008 by Miwatashi et al.,[23] and confirmed that it can serve as a selective A₃AR antagonist across species (≥20-fold selectivity compared with other AR

subtypes).[13] Here we have explored in limited scope the SAR of DPTN for radioisotope incorporation and prepared and characterized a high-affinity tritiated radioligand.

Chemical Synthesis. The synthetic route to **9** followed the original publication[23] with modification and allowed the introduction of a aromatic halogen substitution (Scheme 1). Specifically, a fluorine, bromine, or iodine atom (**16b−d**) was

Scheme 2. Synthesis of Chain-Extended Analogues of 9[a]
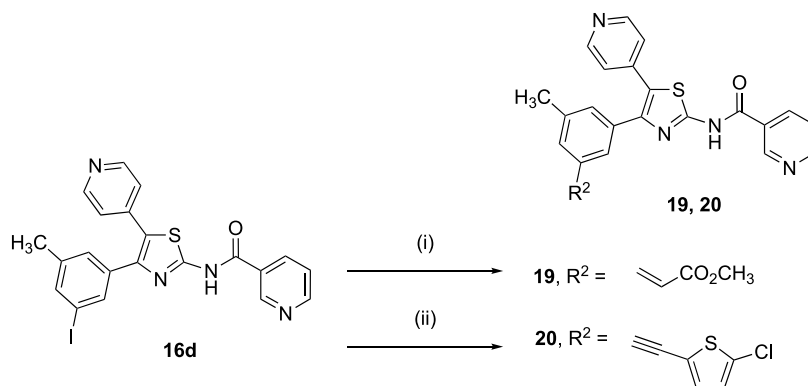
[a]Reagents and conditions: (i) methyl acrylate, Pd(OAc)$_2$ (10 mol %), P(o-tol)$_3$ (10 mol %), DMA, 90 °C, 20 h, 33%; (ii) 5-chloro-thien-2-yl acetylene, Pd(PPh$_3$)$_2$Cl$_2$ (10 mol %), CuI (10 mol %), Et$_3$N, DMF, 80 °C,16 h, 59%.

Table 1. Binding Affinity of Various Known and Newly Synthesized A$_3$AR Antagonists (Affinity at the Human Receptors, Unless Noted; m, Mouse; r, Rat)[a]

compound	A$_1$ (K_i, nM or % at 10 μM)	A$_{2A}$ (K_i, nM or % at 10 μM)	A$_{2B}$ (K_i, nM or % at 10 μM)[b]	A$_3$ (K_i, nM)
6[c]	35.4 ± 4.2%, 27.4 ± 2.0% (m), 25.5 ± 1.9% (r)	16.4 ± 2.9%, 25.1 ± 8.1% (m), 7.4 ± 3.2% (r)	34.5 ± 4.6%, 20.2 ± 5.0% (m), 38.8 ± 4.7% (r)	43.9 ± 7.6, 349 ± 72 (m), 216 ± 65 (r)
9[c]	162 ± 49, 411 ± 113 (m), 333 ± 58 (r)	121 ± 42, 830 ± 92 (m), 1150 ± 80 (r)	230 ± 40, 189 ± 61 (m), 163 ± 23 (r)	1.65 ± 0.57, 9.61 ± 2.27 (m), 8.53 ± 1.22 (r)
16b	78.7 ± 3.3	3550	ND	69.2 ± 11.9
16c	1450 ± 600, 252 ± 64 (m)	−7.3 ± 7.2%, 29 ± 5% (m)	ND	6.34 ± 1.79, 22.3 ± 6.1 (m)
16d	8770 ± 800, 2640 (m)	−15 ± 19%, 7.4 ± 4.2% (m)	ND	6.12 ± 1.92, 12.4 ± 1.6 (m)
17	38 ± 2%	>1000	ND	26.6 ± 7.6
19	1570 ± 390	15 ± 17%	ND	18.9 ± 10.9, 120 (m)
20	21 ± 2%	−0.5 ± 8.9%	ND	80.7 ± 5.8

[a]Radioligands used (concentration): [^{3}H]8-cyclopentyl-1,3-dipropylxanthine ([^{3}H]DPCPX, 21, A$_1$, 0.5 nM), [^{3}H]4-[2-[7-amino-2-(2-furyl)-1,2,4-triazolo[1,5-a][1,3,5]triazin-5-yl-amino]ethyl]phenol ([^{3}H]ZM241385, 22, A$_{2A}$, 1.0 nM) and [^{3}H]21 (A$_{2B}$, 5 nM), and [^{125}I]N6-(4-Amino-3-iodobenzyl)adenosine-5′-N-methyluronamide ([^{125}I]I-AB-MECA 3, A$_3$, 0.1 nM), during 60 min incubations at 25 °C. N-Ethylcarboxamido-adenosine (NECA, 23, 100 μM) was used to define nonspecific binding. [b]ND, not determined. [c]Data from Gao et al.[13]

inserted in the place of a 3-methyl group present in **9**. The inclusion of the Weinreb−Nahm amide **12** leading to the Weinreb ketone[24] **13** provided a higher overall yield than that by the original route. It was possible to acylate arylamine **15** with several nicotinoyl derivatives via their acid chlorides to yield **9** and **17** (Scheme 1B). The tritiated radioligand [^{3}H]**18** ([^{3}H]5-bromo-N-(4-(3,5-dimethylphenyl)-5-(pyridin-4-yl)-thiazol-2-yl)nicotinamide, MRS7799) was synthesized by the catalytic reduction of bromo precursor **17** with tritium gas. [^{3}H]**18** was isolated by HPLC with a specific activity of 23.9 Ci/mmol (stored in an EtOH solution at a concentration of 16.24 μg/mL). The radiochemical purity was 97.5% (Supporting Information).

Compounds **16d** and **17** also served as intermediates for the substitution of functionalized chains at the 3-iodophenyl position (Scheme 2). Heck (**19**) and Sonogashira (**20**) reactions were utilized to install extended, rigidified substituents. These analogues were intended to probe the environment of the A$_3$AR binding site of **9**. If one or more chain-extended analogues would show considerable affinity, then it would enable the design of additional conjugates at those positions. A similar strategy of appending arylethynyl or alkenyl groups to an aromatic ring was successfully applied with 1,4-dihydropyridines as hA$_3$AR antagonists.[13]

We measured the AR affinities of **9** and its analogues (Table 1) using standard radioligand binding assays with radiolabeled A$_1$ and A$_{2A}$ antagonists and an A$_3$ agonist.[12,13,15,25−27] The ARs

were expressed in HEK293 cell membranes, as previously reported. The inhibition constants (K_i) of **9** at the human, mouse, and rat A$_3$ARs were 1.65, 9.61, and 8.53 nM using [^{125}I]**3** as the radioligand.[13] Curiously, unlike most other reported A$_3$AR antagonists, there was moderate affinity of **9** at the A$_{2B}$AR ($K_i \approx$ 200 nM in the three species) and the A$_1$AR and A$_{2A}$AR.[13] Other analogues **16b**−**16d** with halo substitution of the nicotinyl ring were moderately reduced in hA$_3$AR affinity. The rank order of potency for five-position substituents in A$_3$AR binding was: CH$_3$ > I, Br > F. 3-Bromo **16c** and 3-iodo **16d** analogues were 230- and 1400-fold selective, respectively, for hA$_3$AR compared with hA$_1$AR, although the A$_1$AR binding inhibition by **16c** was incomplete (Figure S1, Supporting Information). At the mARs, the 3-iodo derivative **16d** was ~200-fold selective for mA$_3$AR compared with mA$_1$AR. However, 3-fluoro analogue **16b** is a mixed hA$_1$ and hA$_3$AR antagonist. The products of the Heck **19** and Sonogashira **20** reactions were similarly tested in hA$_3$AR binding, and the results indicated the affinity of methyl acrylate derivative **19** to be four times greater than that of 5-chloro-thien-2-yl-ethynyl derivative **20** and only three times less potent than that of the parent **16d**. Compound **19** was 83-fold selective for hA$_3$AR compared with hA$_1$AR and displayed moderate mA$_3$AR affinity. Thus compounds **16c**, **16d**, **17**, and **20** were weaker than the reference antagonist **9** in A$_1$ and A$_{2A}$AR binding, and **16d** was more A$_3$AR-selective than **9**, although it was of lower affinity. The same arylalkyne moiety in
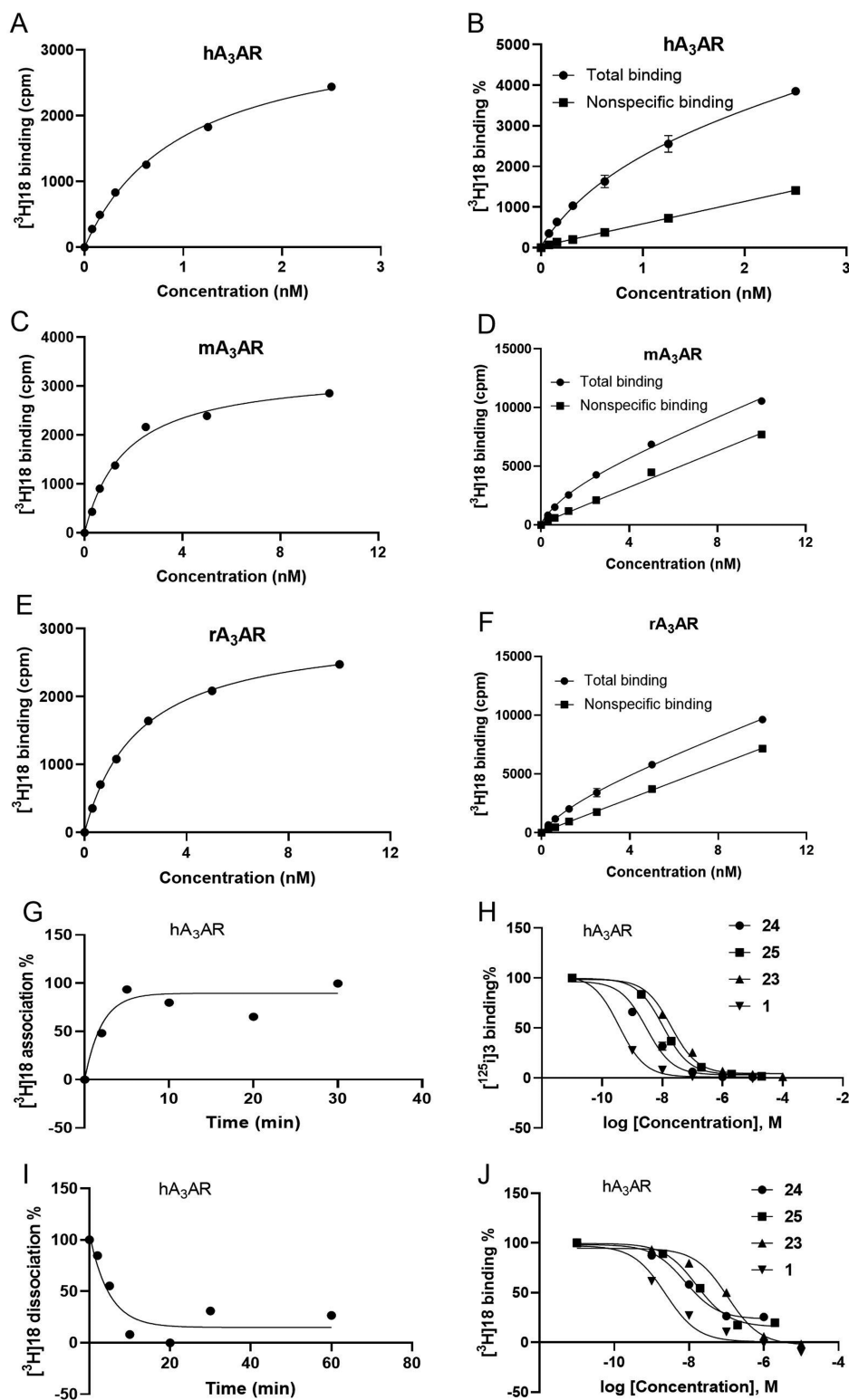
Figure 1. Pharmacology of radioligand $[^3H]$**18** in A_3AR binding saturation, inhibition, and kinetic experiments. Specific binding saturation (A,C,E) and total (●) and nonspecific (■) binding (B,D,F) at three species homologues (human, mouse, rat) of A_3AR expressed in HEK293 cells using 100 μM **23** to define nonspecific binding. Data shown are representative experiments performed in duplicate; the K_d values from four independent experiments are listed in the text. Association (G, k_1 = 0.297 min^{-1}) and dissociation (I, k_{-1} = 0.209 min^{-1}; $t_{1/2}$ = 3.32 min) kinetics of $[^3H]$**18** (1 nM) at the hA$_3$AR. (H,J) Binding inhibition at hA$_3$AR and comparison of $[^3H]$**18** (1 nM) with the agonist radioligand $[^{125}I]$**3** (0.1 nM) as a tracer. Competing ligands were agonists (A$_3$-selective **1**, nonselective **23**) and hA$_3$-selective antagonists (N-[9-chloro-2-(2-furanyl)[1,2,4]triazolo[1,5-c]quinazolin-5-yl]benzeneacetamide, MRS1220 **24**; 1,4-dihydro-2-methyl-6-phenyl-4-(phenylethynyl)-3,5-pyridinedicarboxylic acid 3-ethyl-5-[(3-nitrophenyl)methyl] ester, MRS1334 **25**).[13] K_i values (nM) for the inhibition of antagonist $[^3H]$**18** binding: **24**, 3.24; **25**, 6.49; **23**, 44.1; **1**, 0.96. K_i values (nM) for the inhibition of agonist $[^{125}I]$**3** binding: **24**, 2.97; **25**, 10.6; **23**, 19.6; **1**, 0.37. Corresponding published K_i values for the inhibition of $[^{125}I]$**3** binding: **24**, 0.96 ± 0.32; **25**, 4.58 ± 0.89; **23**, 26; **1**, 1.74 ± 0.36.[13,27,29]
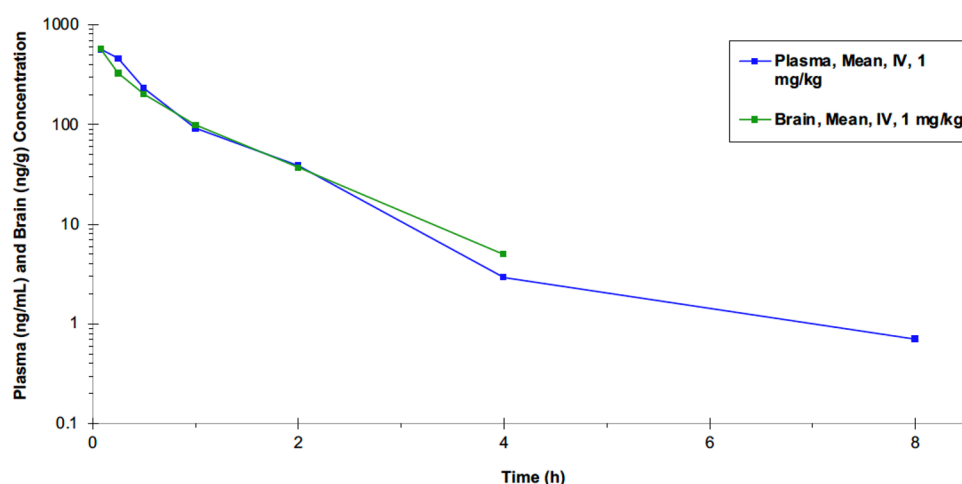
Figure 2. Plasma and brain concentration−time profiles for compound **9** (i.v. bolus, in 10% DMSO/30% PEG400 in 60% PBS, pH 8.5) in male Sprague−Dawley rats.

20 is present at the adenine C2 position of highly potent and selective A_3AR agonists.[12] Similarly, 4-arylalkyne moieties on a 1,4-dihydropyridine scaffold were previously found to induce high hA_3AR-selectivity in antagonists.[1]

The tritiated compound **18** was evaluated as a radiotracer at human, mouse, and rat A_3ARs (Figure 1). Specific binding was saturable at the three species homologues, with the highest level of specific compared with nonspecific binding occurring at the hA_3AR. K_d values determined at A_3ARs in the three species were (nM, $n = 4$): 0.55 ± 0.17 (human), 3.74 ± 0.75 (mouse), and 2.80 ± 0.29 (rat). Association and dissociation rates were determined at the human A_3AR (Figure 1G,I), which provided a kinetic K_d value of 0.76 nM, in close agreement with the other affinity measures of unlabeled **9** and labeled **18**. The binding inhibition by known A_3AR agonists (**1**, **23**) and selective antagonists (**24**, **25**) is shown in Figure 1H,J, in which the use of agonist radioligand $[^{125}I]$**3** was compared with $[^3H]$**18**. The K_i values were comparable to previously determined values, and there was consistency between the two radioligands in antagonist affinity. The incomplete inhibition by antagonists **24** and **25** (Figure 1J) has been previously observed with other hydrophobic antagonists and may be related to a long residence time.[13,28] However, agonists displayed higher affinity using the agonist radioligand compared with $[^3H]$**18**.

Off-target activities of selected antagonist derivatives were measured in radioligand binding assays by the NIMH Psychoactive Drug Screening Program (PDSP).[30] The data are represented as either a K_i value or a % inhibition at 10 μM, if <50%. Compound **9** had no significant binding (>50% inhibition at 10 μM) at any of the 45 receptors, transporters, or channels examined.[13] However, compound **16d** (Table S1, Supporting Information) had several weak binding hits (K_i in μM), that is, at the σ_2 receptor (3.69), TSPO (1.33 $\pm$ 0.23 μM), and D_3 (0.34 $\pm$ 0.06 μM) and D_4 (1.24 $\pm$ 0.02 μM) dopamine receptors. Compound **19** bound to the M_5 muscarinic (3.7 μM) and $5\text{-}HT_{2A}$ (0.96 $\pm$ 0.06 μM) and $5\text{-}HT_{2C}$ (0.79 $\pm$ 0.31 μM) serotonin receptors.

Because one objective was to determine the suitability of this chemical series for PET ligands for A_3AR in vivo brain imaging, we calculated the CNS multiparameter optimization (MPO) score, predictive of crossing the blood−brain barrier (BBB).[31] The score for **9** was 3.81, which indicates possible bioavailability in the brain. Also, on the basis of the criteria of Rankovic et al. (tPSA (topological surface area) of 68 Å^2 and MW 386),[32] the likelihood of crossing the BBB was judged to be >50%. The Lipinski properties were also favorable for potential oral bioavailability (1 HBD, 4 HBA, LogP 4.68).[33]

Therefore, the in vivo pharmacokinetics (PK) of **9** was studied in male Sprague−Dawley rats. The brain distribution of **9** was determined (Figure 2, Table 2) following a bolus

Table 2. PK Parameters in Male Sprague Dawley Rats Following a 1.0 mg/kg Bolus Dose of 9

matrix	C_0 (ng/mL)	C_{avg} (ng/mL)	CL (mL/min/kg)	V_d (L/kg)	$T_{1/2}$ (h)	F_{ub}
plasma	628	52	40	1.8	0.8	0.03
brain	760	95	43	1.9	0.7	0.03

injection of 1 mg/kg (i.v.). A good tissue distribution (V_d) was observed, with moderate-to-high clearance from the body (CL) corresponding to 70% of liver blood flow. There was excellent brain distribution (brain/plasma ratio ~1). However, the compound was highly bound in brain and plasma, with a low free fraction in brain and plasma (Table S2, Supporting Information). The brain/plasma ratio was 1.0 to 1.8. These observations were consistent with a lipophilic compound that readily crosses the BBB.

The estimated percent receptor occupancy of unbound **9** based on the previously published K_i value at the rat A_3AR[23] as a function of time following a 3 mg/kg intravenous dose was close to 100% at early time points (Table S3, Figure S2, Supporting Information). The calculation was performed with no residence time assumptions.

In the absence of an experimental structure, we and others have used hA_3AR homology modeling to predict the binding modes of A_3AR antagonists.[8,12,22,23,26,28,29] Considering the high sequence identity of hA_3AR and hA_1AR (46% full sequence, 56% transmembrane (TM) helices, as reported in GPCRdb[42]), an antagonist-bound X-ray structure of hA_1AR (PDB ID: 5UEN[43]) was used as a template for homology modeling of hA_3AR. In addition, the extracellular loop (EL) 2 was modeled using a previously generated intermediate-state, agonist-bound hA_3AR model as a template, to be consistent with previous works.[44] The same templates were also used to generate a model of mA_3AR, which has high sequence identity

with hA₃AR (72% full sequence, 83% TM). Both hA₃AR and mA₃AR models were refined by minimizing the nonconserved residues and by the induced fit docking of known antagonists: MRS1220 (hA₃AR $K_i \approx 0.7$ nM) and 6 (mA₃AR $K_i \approx 349$ nM) for hA₃AR and mA₃AR,[13] respectively (Figures S4 and S5). The newly generated models show the typical characteristics of inactive ARs as compared with the previously reported intermediate agonist-bound hA₃AR model,[44] such as a translocation of TM3, lack of the bulge of TM5, outward movement of the TM7 intracellular portion and inward movement of the TM5 and TM6 intracellular portions,[46] placing the "toggle switch" W243 (hA₃AR) closer to TM3 (Figure S6).

The obtained models were used to generate a hypothetical binding mode of 9 at the hA₃AR and mA₃AR orthosteric binding sites through docking,[29] and representative docking poses at the two receptors are shown for comparison (Figure 3). The conformations of the human Q167 and V169 and of
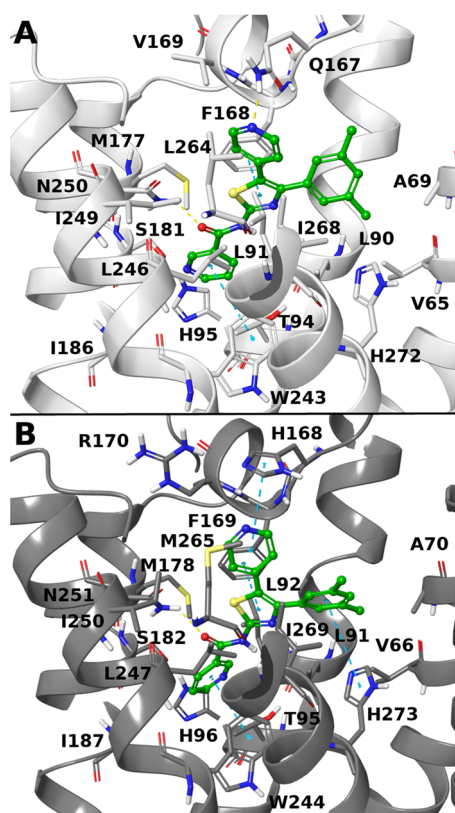
Figure 3. Docking pose of compounds 9 (green) at hA₃AR (white, A) and mA₃AR (gray, B) homology models (coordinate files in Supporting Information). Residues within 3 Å of the ligand are rendered by sticks. Yellow lines indicate H bonds, and cyan lines indicate π−π stacking interactions between the ligand and the receptor.

the murine H168 and R170 were optimized with an induced fit docking procedure. The predicted binding modes of 9 at hA₃AR and mA₃AR are similar, with the thiazole scaffold at the center of the orthosteric binding pocket. The thiazole is involved in a π−π stacking interaction with F168/F169 (hA₃AR/mA₃AR) on EL2 and a hydrophobic contact with L246/L247 on TM6. The sulfur atom is proximal to the carbonyl group of N250/N251 (TM6), which might correspond to an uncommon, but already reported, carbon-

yl−S interaction, although with suboptimal geometry.[45] The nicotinamide is located deep within the binding pocket, where it is surrounded by L90/L91, L91/L92, T94/T95, and H95/H96 on TM3; M177/M178 and I186/I187 on TM5; and W243/W244 and N250/N251 on TM6. The nicotinamide ring appears to be involved in a π−π T-shaped interaction with W243/W244, whereas the amide carbonyl moiety is H-bonded to N250/N251, reflecting the importance of the carbonyl group in this antagonist SAR.[23] The A₃AR affinity-enhancing[23] 4-pyridyl moiety at position five points toward the receptor's extracellular portion in proximity to Q167 (hA₃AR) or H168 and R170 (mA₃AR) on EL2, which can potentially stabilize the pyridyl nitrogen. The aryl group at position four is surrounded by TMs 1, 2, 3, and 7, with a potential π−π stacking with H272/H273 on TM7. The hypothetical binding mode of compound 9 is compatible with the extended methyl acrylate moiety of 19, which maintains considerable binding affinity at both the human ($K_i \approx 18.9$ nM) and mouse ($K_i \approx 120$ nM) receptors. The extended methyl acrylate group of 19 is, in fact, predicted to occupy a cleft between TM2 and TM3 (Figure S7). The rigid extensions at the adenine two position of highly selective A₃AR agonists also are predicted to point toward TM2 when receptor-bound.[12]

In conclusion, compounds 9 and 19 were predicted to bind with a similar conformation at hA₃AR and mA₃AR; in fact, most (~75%) of the residues predicted to be in ligand contact (within 5 Å) are conserved between the two homologues, with the only differences being M66/I67 (TM2), T87/S88 (TM3), L89/V90 (TM3), Q167/H168 (EL2), V169/R170 (EL2), M174/L175 (TM5), I253/S254 (TM6), V259/I260 (EL3), L264/M265 (TM7), and Y265/C266 (TM7).

The G_i-coupled A₃AR is a therapeutic target for inflammatory and ischemic conditions. Although diverse chemotypes have been found as A₃AR-selective antagonists,[18,22,23,25,29,34−37] their utility is mostly limited to higher species.[13] We now report the more complete characterization of a reported antagonist 9 that is less variable across species, including its use as radioligand 18, along with a small set of analogues.

Other thiazole and thiazol-2-amine derivatives have been explored as antagonists of the A₃AR and other ARs.[25,27−30,34−41] Structures of the key reported thiazol-2-amine derivatives that have high hA₃AR affinity in relation to compound 9 are shown in Table S4 (Supporting Information).

Compound 9 is one of the few A₃AR antagonists suitable for use in rodent,[13] and primate species. The only other compound in that category is pyridine derivative 6, but compound 9 is 25, 36, and 27 times more potent than 6 at rat, mouse, and human A₃ARs, respectively. Interestingly, a 3-iodo derivative 16d was shown to be potent and selective for the A₃AR in both humans and mice.

In conclusion, we have expanded the SAR of N-(4-aryl-5-(pyridin-4-yl)thiazol-2-yl)nicotinamides as A₃AR antagonists. Radiolabeling of 9 now provides a useful and versatile radiotracer for binding studies in multiple species, and the unlabeled compound was shown to readily cross the BBB. Our data suggest that this antagonist in both labeled and unlabeled forms will be widely applicable and will fill an unmet need for A₃AR characterization and drug discovery.

ASSOCIATED CONTENT

SI **Supporting Information**

docking pose coordinates (pdb) of (h); molecular formula strings. The Supporting Information is available free of charge at https://pubs.acs.org/doi/10.1021/acsmedchemlett.1c00685.

Chemical synthetic procedures and spectra, PDSP screening results, and molecular modeling methods (PDF)

Docking pose coordinates (pdb) of **9** (h) (PDB)

Docking pose coordinates (pdb) of **9** (m) (PDB)

Docking pose coordinates (pdb) of **24** (h) (PDB)

Docking pose coordinates (pdb) of receptor-bound **6** (m) (PDB)

Molecular formula strings (XLSX)

AUTHOR INFORMATION

Corresponding Author

Kenneth A. Jacobson − *Molecular Recognition Section, Laboratory of Bioorganic Chemistry, National Institute of Diabetes and Digestive and Kidney Diseases, Bethesda, Maryland 20892, United States;* ⓞ orcid.org/0000-0001-8104-1493; Phone: 301-496-9024; Email: kennethj@niddk.nih.gov; Fax: 301-496-8422

Authors

R. Rama Suresh − *Molecular Recognition Section, Laboratory of Bioorganic Chemistry, National Institute of Diabetes and Digestive and Kidney Diseases, Bethesda, Maryland 20892, United States*

Zhan-Guo Gao − *Molecular Recognition Section, Laboratory of Bioorganic Chemistry, National Institute of Diabetes and Digestive and Kidney Diseases, Bethesda, Maryland 20892, United States*

Veronica Salmaso − *Molecular Recognition Section, Laboratory of Bioorganic Chemistry, National Institute of Diabetes and Digestive and Kidney Diseases, Bethesda, Maryland 20892, United States*

Eric Chen − *Molecular Recognition Section, Laboratory of Bioorganic Chemistry, National Institute of Diabetes and Digestive and Kidney Diseases, Bethesda, Maryland 20892, United States*

Ryan G. Campbell − *Molecular Recognition Section, Laboratory of Bioorganic Chemistry, National Institute of Diabetes and Digestive and Kidney Diseases, Bethesda, Maryland 20892, United States*

Russell B. Poe − *Astrocyte Pharmaceuticals, Cambridge, Massachusetts 02142, United States*

Theodore E. Liston − *Astrocyte Pharmaceuticals, Cambridge, Massachusetts 02142, United States*

Complete contact information is available at:

https://pubs.acs.org/10.1021/acsmedchemlett.1c00685

Notes

The authors declare no competing financial interest.

ACKNOWLEDGMENTS

ABBREVIATIONS

AR, adenosine receptor; HEK293, human embryonic kidney 293; DAT, dopamine transporter; GPCR, G-protein-coupled receptor; MD, molecular dynamics; PDSP, NIMH Psychoactive Drug Screening Program; PEG, polyethyleneglycol; PK, pharmacokinetics; rmsd, root-mean-square deviation; SAR, structure−activity relationship; TM, transmembrane helical domain; TSPO, translocator protein.

REFERENCES

(1) Jacobson, K. A.; Merighi, S.; Varani, K.; Borea, P. A.; Baraldi, S.; Aghazadeh Tabrizi, M.; Romagnoli, R.; Baraldi, P. G.; Ciancetta, A.; Tosh, D. K.; Gao, Z.-G.; Gessi, S. A$_3$ adenosine receptors as modulators of inflammation: from medicinal chemistry to therapy. *Med. Res. Rev.* **2018**, *38*, 1031−1072.

(2) Cohen, S.; Stemmer, S. M.; Zozulya, G.; Ochaion, A.; Patoka, R.; Barer, F.; Bar-Yehuda, S.; Rath-Wolfson, L.; Jacobson, K. A.; Fishman, P. CF102 an A$_3$ adenosine receptor agonist mediates anti-tumor and anti-inflammatory effects in the liver. *J. Cell. Physiol.* **2011**, *226*, 2438−2447.

(3) Varani, K.; Vincenzi, F.; Targa, M.; Paradiso, B.; Parrilli, A.; Fini, M.; Lanza, G.; Borea, P. A. The stimulation of A$_3$ adenosine receptors reduces bone-residing breast cancer in a rat preclinical model. *Eur. J. Cancer.* **2013**, *49*, 482−491.

(4) Ranjan, A.; Iyer, S. V.; Iwakuma, T. Suppressive roles of A$_3$AR and TMIGD3 i1 in osteosarcoma malignancy. *Cell Cycle* **2017**, *16* (10), 903−904.

(5) Iannone, R.; Miele, L.; Maiolino, P.; Pinto, A.; Morello, S. Adenosine limits the therapeutic effectiveness of anti-CTLA4 mAb in a mouse melanoma model. *Am. J. Cancer Res.* **2014**, *4*, 172−181.

(6) Fishman, P.; Cohen, S. The A$_3$ adenosine receptor (A$_3$AR): therapeutic target and predictive biological marker in rheumatoid arthritis. *Clin. Rheumatol.* **2016**, *35*, 2359−2362.

(7) Little, J.; Ford, A.; Symons-Liguori, A. M.; Chen, Z.; Janes, K.; Doyle, T.; Xie, J.; Luongo, L.; Tosh, D.; Maione, S.; Bannister, K.; Dickenson, A.; Vanderah, T. W.; Porreca, F.; Jacobson, K. A.; Salvemini, D. Endogenous adenosine A$_3$ receptor activation selectively alleviates persistent pain states. *Brain* **2015**, *138*, 28−35.

(8) Antonioli, L.; Lucarini, E.; Lambertucci, C.; Fornai, M.; Pellegrini, C.; Benvenuti, L.; Di Cesare Mannelli, L.; Spinaci, A.; Marucci, G.; Blandizzi, C.; Ghelardini, C.; Volpini, R.; Dal Ben, D. The anti-inflammatory and pain-relieving effects of AR170, an adenosine A$_3$ receptor agonist, in a rat model of colitis. *Cells* **2020**, *9* (6), 1509.

(9) Fishman, P.; Cohen, S.; Itzhak, I.; Amer, J.; Salhab, A.; Barer, F.; Safadi, R. The A$_3$ adenosine receptor agonist, namodenoson, ameliorates non-alcoholic steatohepatitis in mice. *Int. J. Mol. Med.* **2019**, *44*, 2256−2264.

(10) Li, P.; Li, X.; Deng, P.; Wang, D.; Bai, X.; Li, Y.; Luo, C.; Belguise, K.; Wang, X.; Wei, X.; Xia, Z.; Yi, B. Activation of adenosine A$_3$ receptor reduces early brain injury by alleviating neuro-inflammation after subarachnoid hemorrhage in elderly rats. *Aging (Albany NY)* **2021**, *13*, 694−713.

(11) Liston, T. E.; Hinz, S.; Müller, C. E.; Holstein, D. M.; Wendling, J.; Melton, R. J.; Campbell, M.; Korinek, W. S.; Suresh, R. R.; Sethre-Hofstad, D.; Gao, Z. G.; Tosh, D. K.; Jacobson, K. A.; Lechleiter, J. D. Nucleotide P2Y$_1$ receptor agonists are *In vitro* and *In vivo* prodrugs of A$_1$/A$_3$ adenosine receptor agonists: Implications for roles of P2Y$_1$ and A$_1$/A$_3$ receptors in health and disease. *Purinergic Signalling* **2020**, *16*, 543−559.

(12) Tosh, D. K.; Salmaso, V.; Rao, H.; Campbell, R.; Bitant, A.; Gao, Z. G.; Auchampach, J. A.; Jacobson, K. A. Direct comparison of

(N)-methanocarba and ribose-containing 2-arylalkynyladenosine derivatives as A$_3$ receptor agonists. *ACS Med. Chem. Lett.* **2020**, *11*, 1935−1941.

(13) Gao, Z. G.; Suresh, R. R.; Jacobson, K. A. Pharmacological characterization of DPTN and other selective A$_3$ adenosine receptor antagonists. *Purinergic Signalling* **2021**, *17*, 737−746.

(14) Leung, C. T.; Li, A.; Banerjee, J.; Gao, Z. G.; Kambayashi, T.; Jacobson, K. A.; Civan, M. M. The role of activated adenosine receptors in degranulation of human LAD2 mast cells. *Purinergic Signalling* **2014**, *10*, 465−475.

(15) Gao, Z. G.; Blaustein, J.; Gross, A. S.; Melman, N.; Jacobson, K. A. N^6-Substituted adenosine derivatives: Selectivity, efficacy, and species differences at A$_3$ adenosine receptors. *Biochem. Pharmacol.* **2003**, *65*, 1675−1684.

(16) Yang, J. N.; Wang, Y.; Garcia-Roves, P. M.; Bjornholm, M.; Fredholm, B. B. Adenosine A$_3$ receptors regulate heart rate, motor activity and body temperature. *Acta Physiol* **2010**, *199*, 221−230.

(17) Olah, M. E.; Gallo-Rodriguez, C.; Jacobson, K. A.; Stiles, G. L. ^{125}I-4-Aminobenzyl-5′-N-methylcarboxamidoadenosine, a high affinity radioligand for the rat A$_3$ adenosine receptor. *Mol. Pharmacol.* **1994**, *45*, 978−982.

(18) Yang, X.; Heitman, L. H.; IJzerman, A. P.; van der Es, D. Molecular probes for the human adenosine receptors. *Purinergic Signalling* **2021**, *17*, 85−108.

(19) Gao, Z. G.; Teng, B.; Wu, H.; Joshi, B. V.; Griffiths, G. L.; Jacobson, K. A. Synthesis and pharmacological characterization of [^{125}I]MRS1898, a high affinity, selective radioligand for the rat A$_3$ adenosine receptor. *Purinergic Signalling* **2009**, *5*, 31−37.

(20) Alnouri, M. W.; Jepards, S.; Casari, A.; Schiedel, A. C.; Hinz, S.; Müller, C. E. Selectivity is species-dependent: Characterization of standard agonists and antagonists at human, rat, and mouse adenosine receptors. *Purinergic Signalling* **2015**, *11* (3), 389−407.

(21) Balber, T.; Singer, J.; Berroterán-Infante, N.; Dumanic, M.; Fetty, L.; Fazekas-Singer, J.; Vraka, C.; Nics, L.; Bergmann, M.; Pallitsch, K.; Spreitzer, H.; Wadsak, W.; Hacker, M.; Jensen-Jarolim, E.; Viernstein, H.; Mitterhauser, M. Preclinical In Vitro and In Vivo evaluation of [^{18}F]FE@SUPPY for cancer PET imaging: Limitations of a xenograft model for colorectal cancer. *Contrast Media Molecular Imaging* **2018**, *2018*, 1−9.

(22) Barkan, K.; Lagarias, P.; Stampelou, M.; Stamatis, D.; Hoare, S.; Safitri, D.; Klotz, K.-N.; Vrontaki, E.; Kolocouris, A.; Ladds, G. Pharmacological characterisation of novel adenosine A$_3$ receptor antagonists. *Sci. Rep.* **2020**, *10*, 20781.

(23) Miwatashi, S.; Arikawa, Y.; Matsumoto, T.; Uga, K.; Kanzaki, N.; Imai, Y. N.; Ohkawa, S. Synthesis and biological activities of 4-phenyl-5-pyridyl-1,3-thiazole derivatives as selective adenosine A$_3$ antagonists. *Chem. Pharm. Bull. (Tokyo)* **2008**, *56* (8), 1126−1137.

(24) Nahm, S.; Weinreb, S. M. N-methoxy-N-methylamides as effective acylating agents. *Tetrahedron Lett.* **1981**, *22* (39), 3815−3818.

(25) Jung, K.-Y.; Kim, S.-K.; Gao, Z.-G.; Gross, A. S; Melman, N.; Jacobson, K. A; Kim, Y.-C. Structure activity relationships of thiazole and thiadiazole derivatives as potent adenosine A$_3$ receptor antagonists. *Bioorg. Med. Chem.* **2004**, *12*, 613−623.

(26) Tosh, D. K.; Salmaso, V.; Rao, H.; Bitant, A.; Fisher, C. L.; Lieberman, D. I.; Vorbrüggen, H.; Reitman, M. L.; Gavrilova, O.; Gao, Z. G.; Auchampach, J. A.; Jacobson, K. A. Truncated (N)-methanocarba nucleosides as partial agonists at mouse and human A$_3$ adenosine receptors: Affinity enhancement by N^6-(2-phenylethyl) substitution. *J. Med. Chem.* **2020**, *63*, 4334−4348.

(27) Melman, A.; Gao, Z. G.; Kumar, D.; Wan, T. C.; Gizewski, E.; Auchampach, J. A.; Jacobson, K. A. Design of (N)-methanocarba adenosine 5′-uronamides as species-independent A$_3$ receptor-selective agonists. *Bioorg. Med. Chem. Lett.* **2008**, *18*, 2813−2819.

(28) Xia, L.; Burger, W. A. C.; van Veldhoven, J. P. D.; Kuiper, B. J.; van Duijl, T. T.; Lenselink, E. B.; Paasman, E.; Heitman, L. H.; IJzerman, A. P. Structure-affinity relationships and structure-kinetics relationships of pyrido[2,1-f]purine-2,4-dione derivatives as human

adenosine A$_3$ receptor antagonists. *J. Med. Chem.* **2017**, *60* (17), 7555−7568.

(29) Jacobson, K. A.; Tosh, D. K.; Gao, Z.-G.; Yu, J.; Suresh, R. R.; Rao, H.; Romagnoli, R.; Baraldi, P. G.; Aghazadeh Tabrizi, M. Chapter 7. Medicinal chemistry of the A$_3$ adenosine receptor. *The Adenosine Receptors, The Receptors* **2018**, *34*, 169−198.

(30) Besnard, J.; Ruda, G. F.; Setola, V.; Abecassis, K.; Rodriguiz, R. M.; Huang, X.-P.; Norval, S.; Sassano, M. F.; Shin, A. I.; Webster, L. A.; Simeons, F. R. C.; Stojanovski, L.; Prat, A.; Seidah, N. G.; Constam, D. B.; Bickerton, G. R.; Read, K. D.; Wetsel, W. C.; Gilbert, I. H.; Roth, B. L.; Hopkins, A. L. Automated design of ligands to polypharmacological profiles. *Nature* **2012**, *492*, 215−220.

(31) Wager, T. T.; Hou, X.; Verhoest, P. R.; Villalobos, A. Moving beyond rules: the development of a central nervous system multiparameter optimization (CNS MPO) approach to enable alignment of druglike properties. *ACS Chem. Neurosci.* **2010**, *1*, 435−439.

(32) Rankovic, Z. Retraction of "CNS Physicochemical Property Space Shaped by a Diverse Set of Molecules with Experimentally Determined Exposure in the Mouse Brain". *J. Med. Chem.* **2019**, *62* (3), 1699.

(33) Benet, L. Z.; Hosey, C. M.; Ursu, O.; Oprea, T. I. BDDCS, the Rule of 5 and drugability. *Adv. Drug Delivery Rev.* **2016**, *101*, 89−98.

(34) Press, N.; Keller, T.; Tranter, P.; Beer, D.; Jones, K.; Faessler, A.; Heng, R.; Lewis, C.; Howe, T.; Gedeck, P. New highly potent and selective adenosine A$_3$ receptor antagonists. *Curr. Top. Med. Chem.* **2004**, *4*, 863−870.

(35) Abdelrahman, A.; Yerande, S. G.; Namasivayam, V.; Klapschinski, T. A.; Alnouri, M. W.; El-Tayeb, A.; Müller, C. E. Substituted 4-phenylthiazoles: Development of potent and selective A$_1$, A$_3$ and dual A$_1$/A$_3$ adenosine receptor antagonists. *Eur. J. Med. Chem.* **2020**, *186*, 111879.

(36) Pandya, D. H.; Sharma, J. A.; Jalani, H. B.; Pandya, A. N.; Sudarsanam, V.; Kachler, S.; Klotz, K. N.; Vasu, K. K. Novel thiazole-thiophene conjugates as adenosine receptor antagonists: synthesis, biological evaluation and docking studies. *Bioorg. Med. Chem. Lett.* **2015**, *25* (6), 1306−1309.

(37) Yaziji, V.; Rodríguez, D.; Gutiérrez-De-Terán, H.; Coelho, A.; Caamaño, O.; García-Mera, X.; Brea, J.; Loza, M. I.; Cadavid, M. I.; Sotelo, E. Pyrimidine derivatives as potent and selective A$_3$ adenosine receptor antagonists. *J. Med. Chem.* **2011**, *54* (2), 457−471.

(38) Webb, T. R.; Melman, N.; Lvovskiy, D.; Ji, X. d.; Jacobson, K. A. The utilization of a unified pharmacophore query in the discovery of new antagonists of the adenosine receptor family. *Bioorg. Med. Chem. Lett.* **2000**, *10*, 31−34.

(39) van Muijlwijk-Koezen, J. E.; Timmerman, H.; Vollinga, R. C.; Frijtag von Drabbe Kunzel, J.; de Groote, M.; Visser, S.; IJzerman, A. P. Thiazole and thiadiazole analogues as a novel class of adenosine receptor antagonists. *J. Med. Chem.* **2001**, *44*, 749−762.

(40) Inamdar, G. S.; Pandya, A. N.; Thakar, H. M.; Sudarsanam, V.; Kachler, S.; Sabbadin, D.; Moro, S.; Klotz, K.-N.; Vasu, K. K. New insight into adenosine receptors selectivity derived from a novel series of [5-substituted-4-phenyl-1,3-thiazol-2-yl] benzamides and fura-mides. *Eur. J. Med. Chem.* **2013**, *63*, 924−934.

(41) Trifilieff, A.; Keller, T. H.; Press, N. J.; Howe, T.; Gedeck, P.; Beer, D.; Walker, C. CGH2466, a combined adenosine receptor antagonist, p38 mitogen-activated protein kinase and phosphodiesterase type 4 inhibitor with potent in vitro and in vivo anti-inflammatory activities. *Br. J. Pharmacol.* **2005**, *144* (7), 1002−1010.

(42) Pándy-Szekeres, G.; Munk, C.; Tsonkov, T. M.; Mordalski, S.; Harpsøe, K.; Hauser, A. S.; Bojarski, A. J.; Gloriam, D. E. GPCRdb in 2018: adding GPCR structure models and ligands. *Nucleic Acids Res.* **2018**, *46*, D440−D446.

(43) Glukhova, A.; Thal, D. M.; Nguyen, A. T.; Vecchio, E. A.; Jörg, M.; Scammells, P. J.; May, L. T.; Sexton, P. M.; Christopoulos, A. Structure of the adenosine A$_1$ receptor reveals the basis for subtype selectivity. *Cell* **2017**, *168*, 867−877.

(44) Tosh, D. K.; Salmaso, V.; Rao, H.; Bitant, A.; Fisher, C. L.; Lieberman, D. I.; Vorbrüggen, H.; Reitman, M. L.; Gavrilova, O.;

Gao, Z.-G.; Auchampach, J. A.; Jacobson, K. A. Truncated (N)-methanocarba nucleosides as partial agonists at mouse and human A_3 adenosine receptors: Affinity enhancement by N^6-(2-phenylethyl) substitution. *J. Med. Chem.* **2020**, *63*, 4334−4348.

(45) Beno, B. R.; Yeung, K.-S.; Bartberger, M. D.; Pennington, L. D.; Meanwell, N. A. A survey of the role of noncovalent sulfur interactions in drug design. *J. Med. Chem.* **2015**, *58*, 4383−4438.

(46) Carpenter, B.; Lebon, G. Human adenosine A_{2A} receptor: molecular mechanism of ligand binding and activation. *Front. Pharmacol.* **2017**, *8*, 898.